Arch. Metall. Mater. **71** (2026), 2, 527-530

DOI: https://doi.org/10.24425/amm.2026.158834

JOON PHIL CHOI[1*], YONGRAE KIM[1], DONGWOON SHIN[1], MIN-KYO JUNG[1], PIL-HO LEE[1], HYUN-GON LYU[2], JOON-CHUL YUN[2]

EFFECT OF WASHING PROCESS ON THE MAGNETIC PROPERTY OF Sm_2Fe_{17} NANOPOWDER PREPARED BY MODIFIED REDUCTION-DIFFUSION PROCESS

This study investigates the influence of an improved washing process on the magnetic properties of Sm_2Fe_{17} nanopowders synthesized via modified reduction-diffusion (MRD) process. In particular, hydrazine (N_2H_4) was used to reduce dissolved oxygen in deionized (DI) water, aiming to minimize oxidation during the removal of byproduct CaO. Compared to conventional DI water washing, the N_2H_4-treated process significantly reduced the oxygen content in the nanopowder from 2.53 wt.% to 0.85 wt.%, while also lowering residual Ca from 0.56 wt.% to 0.32 wt.%. As a result, the saturation magnetization (M_s) increased significantly from 73.9 emu/g to 127 emu/g, and coercivity (H_c) remained stable around 1150 Oe. These results highlight the critical role of wash water chemistry in preserving the intrinsic magnetic performance of Sm_2Fe_{17} nanopowders and optimizing their suitability for permanent magnet applications.

Keywords: Sm_2Fe_{17} nanopowder; Washing process; Reduction-diffusion process; Magnetic property

1. Introduction

$Sm_2Fe_{17}N_x$-based magnetic materials have attracted attention as promising permanent magnet materials due to their strong uniaxial magnetic anisotropy, high saturation magnetization, and excellent corrosion resistance, following Nd-Fe-B magnets [1]. However, $Sm_2Fe_{17}N_x$, which has a Curie temperature (T_c) of approximately 470°C, undergoes phase separation into SmN and α-Fe at temperatures exceeding 600°C, limiting its applicability in sintered magnets [2]. Currently, commercial $Sm_2Fe_{17}N_x$ permanent magnets are typically fabricated as bonded magnets by blending the powder with rubber or polymer binders for injection or compression molding. Attempts to develop sintered $Sm_2Fe_{17}N_x$ magnets by various sintering methods (i.e., hot pressing, HIP, pulsed electric current sintering) have encountered challenges, including the difficulty of shaping and limited mass production [3,4]. Alternatively, using nanoscale $Sm_2Fe_{17}N_x$ powders offers advantages such as enhanced coercivity and increased surface area, which can improve sintering kinetics at lower temperatures.

$Sm_2Fe_{17}N_x$ powders are typically synthesized by nitriding Sm_2Fe_{17} precursors made by melting or reduction-diffusion process [5-8]. The particle size of the final $Sm_2Fe_{17}N_x$ powder depends considerably on that of the Sm_2Fe_{17} precursor, making nanoscale refinement a crucial step [6]. Yun et al. [9,10] have proposed a modified reduction-diffusion (MRD) process to produce stable Sm_2Fe_{17} nanopowders below 800°C via reduction of Sm_2O_3 by CaH_2, followed by diffusion of reduced Sm into nanoscale Fe particles. However, the powders contain byproduct CaO, usually removed by washing with deionized (DI) water – yet this can oxidize Sm_2Fe_{17} powders and degrade their magnetic properties [11]. This study examines how the washing process affects the magnetic properties and composition of Sm_2Fe_{17} nanopowders produced by the MRD process, focusing on reducing oxidation via an improved washing method.

2. Experimental

The precursor powders for the MRD process were Sm_2O_3 (Kojundo, 99.9%, 1 μm), Fe_2O_3 (Kojundo, 99.9%, 1 μm), and CaH_2 (Junsei Chemical, 94%) as the solid reducing agent. Powder preparation proceeded in two steps. First, Sm_2O_3 (1.07 × stoichiometric) and Fe_2O_3 (1.0 × stoichiometric) were SPEX milled at 1060 cycles/min for 1 h to form a Sm_2O_3-Fe_2O_3 mixture, then reduced in H_2 at 450°C for 50 min to obtain Sm_2O_3-

[1] DEPARTMENT OF 3D PRINTING, KOREA INSTITUTE OF MACHINERY & MATERIALS, DAEJEON, REPUBLIC OF KOREA
[2] POWDER TECHNOLOGY DEVELOPMENT TEAM, HYUNDAI-STEEL COMPANY, DANGJIN, REPUBLIC OF KOREA
* Corresponding author: jpchoi@kimm.re.kr

Fe powder [12]. In the second step, CaH_2 (4.5 × stoichiometric) was added and SPEX milled under Ar for 1 h. The resulting powder was heated at 700°C for 3 h in Ar-5%H_2, followed by 2 h under vacuum (1 Pa), and then cooled to room temperature. The heat-treated powder was washed with DI water to remove residual CaO. The detailed MRD process was demonstrated in our previous study [10].

The phase composition of the powders was analyzed using X-ray diffraction (XRD, Rigaku D/MAX-2500/PC) with Cu Kα radiation (λ = 1.54056 Å) over a 2θ range of 20-90° at a scan speed of 4°/min. The microstructure of the powders was examined using scanning electron microscopy (SEM) and transmission electron microscopy (TEM). The magnetic properties, including coercivity and saturation magnetization, were measured using a vibrating sample magnetometer (VSM, Lakeshore VSM 7400) under a maximum applied field of 15 kOe. The elemental composition was analyzed using inductively coupled plasma atomic emission spectroscopy (ICP-AES, Spectro ARCOS) and nitrogen/oxygen analyzer (N/O, Leco TC-600).

3. Results and discussion

Fig. 1(a) shows the microstructure of Sm_2O_3-Fe powder prepared during the first step of microstructure control, as described in the experimental procedures. The powder formed aggregates of approximately 5-20 μm in size, each consisting of particles only a few tens of nanometers in diameter. XRD analysis confirmed that the powder mixture contained both Sm_2O_3 and Fe phases (Fig. 1(b)). Fig. 1(c) illustrates the microstructure of Sm_2O_3-Fe-CaH_2 powder obtained after the second step of microstructure control, revealing spherical aggregates approximately 5-10 μm in size, composed of nano-sized particles. Through the two-step preparation, the resulting mixed milled powder exhibited uniformly distributed nanoscale Sm_2O_3, Fe, and CaH_2 particles. As shown in Fig. 1(d), XRD analysis

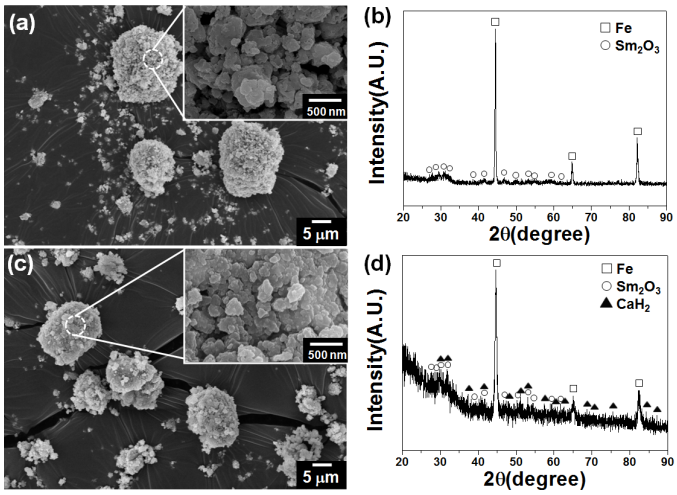

Fig. 1. SEM micrographs of (a) Sm_2O_3-Fe mixture powder in the first step and (c) Sm_2O_3-Fe-CaH_2 mixture powder in the second step of microstructure control for the starting powders. (b) and (d) show the corresponding XRD patterns of (a) and (c), respectively

indicated that the mixed powder retained Fe, Sm_2O_3, and CaH_2 phases, with no observable phase changes in CaH_2 throughout the powder preparation, which was conducted under a protective Ar atmosphere [13].

Fig. 2 presents the XRD-based phase analyses of the powders before and after washing, following the MRD process performed at 700°C using the mixed powders shown in Fig. 1. Prior to washing, strong diffraction peaks corresponding to Sm_2Fe_{17}, along with byproduct CaO and residual Fe, were observed (Fig. 2(a)). In general, Sm_2Fe_{17} powders produced through the MRD process were formed predominantly via two main steps: 1) under Ar-5%H_2 atmosphere Sm_2O_3 was reduced to SmH_2, 2) under a 1 Pa vacuum atmosphere, the SmH_2 decomposed, and Sm diffused into the Fe matrix to form the Sm_2Fe_{17} phase [9]. After the synthesized powder was washed with distilled water, the byproduct CaO was successfully removed (Fig. 2(b)) [8]. Compared to Fig. 2(a), XRD analysis of Fig. 2(b) more clearly revealed residual Fe peaks. By calculating the volume fractions of Sm_2Fe_{17} (303) and Fe (110) [14], the ratio was Sm_2Fe_{17}: Fe = 84%: 16%. A critical consideration in producing Sm_2Fe_{17} powders via reduction-diffusion is achieving a single Sm_2Fe_{17} phase without residual Sm_2O_3 or Fe [11]. However, 16% unreacted Fe was observed in this study, likely due to powder losses during dry mixing and milling – an issue that can be minimized by adjusting the powder preparation [11,15].

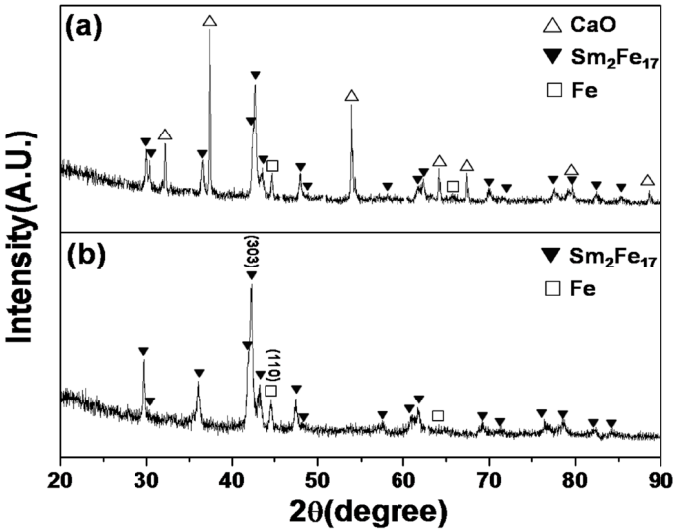

Fig. 2. XRD patterns of the MRD processed powder: (a) as-processed and (b) after the washing process

Fig. 3 shows SEM and TEM analyses of the prepared powders. The SEM micrograph (Fig. 3(a)) revealed particles primarily in the size range of 100-300 nm, consistent with the TEM observation (Fig. 3(b)). Selected Area Electron Diffraction (SAED) patterns further confirmed the presence of the Sm_2Fe_{17} phase, aligning with the XRD results. Overall, these structural analyses confirm the formation of the rhombohedral Th_2Zn_{17}-type (2:17R) structure [16]. Although Sm_2Fe_{17} precursor powders are not typically studied in detail for their magnetic properties prior to nitriding, certain references do provide comparative metrics.

For instance, Isnard et al. [17] reported a saturation magnetization (M_s) of 133 emu/g at –270°C and 117 emu/g at room temperature for Sm_2Fe_{17} (<25 μm) produced by induction melting. Coercivity (H_c) in Sm_2Fe_{17}-based compounds strongly depends on particle size [18]. Fig. 4 displays hysteresis loops of Sm_2Fe_{17} nanopowder at room temperature. The sample synthesized via the MRD process (black line) exhibited a measured M_s (73.9 emu/g), which is significantly lower than the reference value of 117 emu/g. This reduction can be attributed to compositional deviations resulting from non-magnetic impurities such as residual Ca, CaO, or oxidized phases introduced during the washing process [19]. Meanwhile, the measured H_c reached 1250 Oe, substantially higher than the 310 Oe reported in a previous study for Sm_2Fe_{17} powders larger than 10 μm [20]. This enhancement in H_c aligns with the reduced particle size, which limits pathways for domain wall propagation.

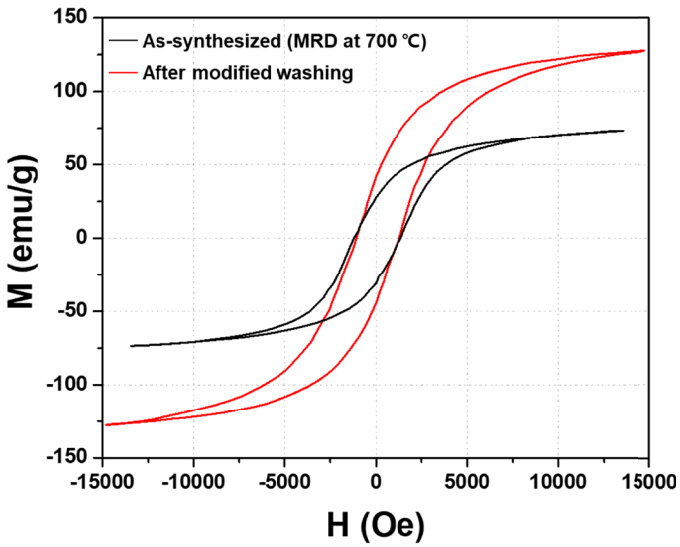

Fig. 3. Microstructure of the MRD processed powder: (a) SEM and (b) TEM

To clarify the low M_s from VSM measurements, compositional analyses of Sm_2Fe_{17} powder were conducted. ICP analysis was used to quantify the Sm, Fe, and Ca contents, while oxygen concentration was determined using a N/O analyzer. Theoretically, Sm_2Fe_{17} should contain 24.05 wt.% Sm and 75.95 wt.% Fe [11]. The synthesized powder had 24.45 wt.% Sm and 74.99 wt.% Fe, closely aligned with the target stoichiometry. However, the Ca content was relatively high (0.56 wt.%), compared to 0.11 wt.% reported in the conventional reduction-diffusion process. Additionally, the oxygen content reached 2.53 wt.%, more than three times higher than the 0.72 wt.% from micron-sized Sm_2Fe_{17} powder. This phenomenon can be attributed to the increased surface area of nanoscale powders, which elevates their reactivity compared to micron-sized powders. This high oxygen content considerably influences the overall composition of Sm_2Fe_{17} powder and is considered a key factor in the reduced M_s value observed in Fig. 4.

Hydrazine (N_2H_4) is known to remove dissolved oxygen from distilled water [21]. Although removing 80 ml of dissolved oxygen theoretically requires 80 ml of N_2H_4 per liter of water, an approximate fourfold excess (320 ml) is often more effective. In this study, 320 ml of hydrazine hydrate ($N_2H_4 \cdot H_2O$, 80 wt.%) was added to 1 liter of distilled water and stirred for about 5 min to remove dissolved oxygen, tracked by a Dissolved Oxygen meter (Hanna Instruments, HI9145). As summarized in TABLE 1, the oxygen decreased from 6.82 ppm to 3.17 ppm following the treatment. While complete removal of dissolved oxygen is challenging due to continuous exposure of air, the achieved value is considered sufficient for practical washing purposes. This is further supported by industrial standards [21], where dissolved oxygen levels in electronic and electrical applications typically range from 13.7% to 41.1%.

TABLE 1

Dissolved oxygen content changes of DI water for the washing process

Samples	Dissolved oxygen content	
	PPM	%
Air	9.07	100
DI water	6.82	75
DI water with N_2H_4	3.17	35

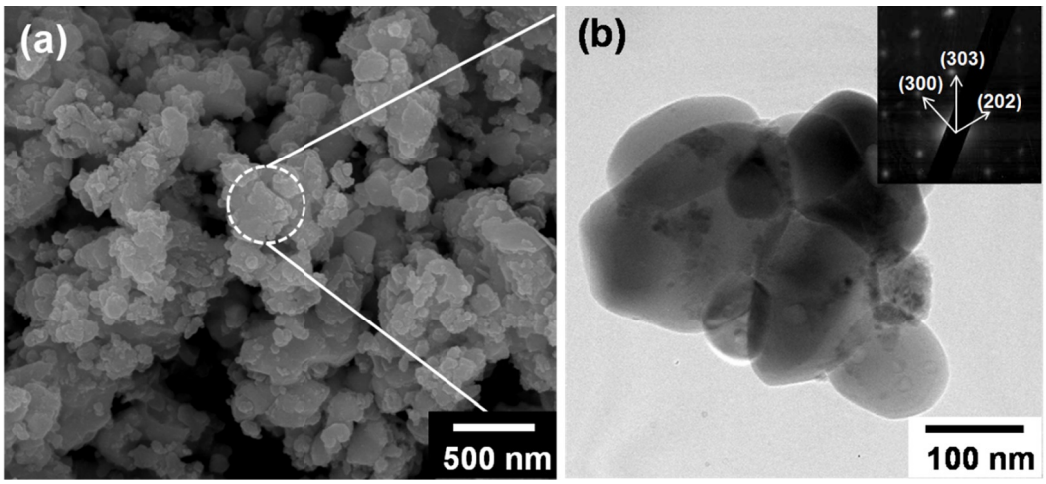

Fig. 4. Hysteresis loops of Sm_2Fe_{17} nanopowders synthesized by MRD process at 700°C and after the modified washing process

Using this de-oxygenated water, the washing process was repeated 3-5 times, followed by an acetone rinse and drying at 50°C to remove residual moisture. Fig. 4(b) presents the magnetic properties of the Sm_2Fe_{17} nanopowder prepared using the improved washing method. The measured M_s reached 127 emu/g, which is not only significantly higher than the previous value of 73.9 emu/g but also exceeds the reference value of 117 emu/g. Konishi et al. [22] reported that residual Fe in Sm_2Fe_{17} powders can increase overall M_s due to its higher intrinsic magnetization (200 emu/g) compared to that of Sm_2Fe_{17} (117 emu/g). Given the presence of approximately 16% residual Fe, as shown in Fig. 2, the observed M_s value exceeding that of pure Sm_2Fe_{17} is considered reasonable. The volume fractions of Sm_2Fe_{17} and Fe were converted into mass fractions using well-established equations [23], and these values were then applied in Eq. (1) to calculate the total M_s value. In this calculation, the M_s values for Sm_2Fe_{17} and Fe were assumed to be 117 emu/g and 200 emu/g, respectively [24]. The resulting M_s, accounting for residual Fe, was approximately 131 emu/g – closely matching the measured value of 127 emu/g. Although residual Fe enhances magnetization, it may also impede uniform nitriding during subsequent $Sm_2Fe_{17}N_x$ formation; therefore, further studies are recommended to clarify its effects on nitrogen absorption and the resulting structural and magnetic properties.

$$Total\, M_s = 117 W_{Sm_2Fe_{17}} + 200 W_{Fe} \quad (1)$$

where $W_{Sm_2Fe_{17}}$ and W_{Fe} represent the mass fractions of the Sm_2Fe_{17} and α-Fe phases, respectively.

Despite the improvement in M_s, the H_c remained around 1150 Oe, indicating that H_c is primarily governed by particle size. ICP and N/O analyses of the Sm_2Fe_{17} nanopowder prepared using the improved method showed that the Sm and Fe contents were 23.85 wt.% and 75.83 wt.%, respectively – closely matching the theoretical values. The Ca content was reduced to 0.32 wt.%, lower than the previously measured 0.56 wt.%. Notably, the oxygen content decreased substantially to 0.85 wt.%, representing an approximate 70% reduction compared to the 2.53 wt.% observed with the conventional washing method. This reduction in oxygen content, achieved by removing dissolved oxygen with N_2H_4, effectively minimized oxidation reactions in the Sm_2Fe_{17} nanopowder.

4. Conclusions

In this study, Sm_2Fe_{17} nanopowders were successfully synthesized at 700°C by the MRD process, forming a stable rhombohedral Th_2Zn_{17}-type structure with particle sizes around 100-300 nm. Conventional DI water washing caused significant oxidation, yielding 2.53 wt.% O and a low M_s of 73.9 emu/g. In contrast, hydrazine-treated DI water reduced the oxygen content to 0.85 wt.%, raising M_s to 127 emu/g while maintaining an H_c of 1152 Oe. These results confirm that controlling the washing process is essential for optimizing the magnetic properties of Sm_2Fe_{17} nanopowders for permanent magnet applications.

Acknowledgments

This study was supported by the Basic Research Program funded by the Korea Institute of Machinery & Materials (KIMM) (No. NK263B) and the Technology Innovation Program funded by the Ministry of Trade, Industry, and Energy (MOTIE, Korea) (No. RS-2024–00441774).

REFERENCES

[1] J.M.D. Coey, H. Sun, J. Magn. Mater. **87**, L251 (1990).
[2] K.M. Zuek, P.J. Guiness, G. Drazic, J. Alloys Comp. **345**, 214 (2002).
[3] K. Machida, Y. Nakatani, G. Adachi, A. Onodera, Appl. Phys. Lett. **62**, 2874 (1993).
[4] S. Ito, M. Kikuchi, T. Fujii, T. Ishikawa, J. Magn. Magn. Mater. **270**, 15 (2004).
[5] C.J. Yang, W.Y. Lee, H.S. Shin, J. Appl. Phys. **74**, 6824 (1993).
[6] M.Z. Su, S.F. Liu, X.L. Qian, J.H. Kin, J. Alloys Comp. **249**, 229 (1997).
[7] Y. Kawano, M. Kume, K. Ichinomiya: United States Patent, US 20020029824 A1 (2002).
[8] R.E. Cech, N.Y. Scotia: United States Patent, US 3748193 (1973).
[9] J.C. Yun, J.S. Lee, J. Ceram. Process Res. **13**, 215 (2012).
[10] J.C. Yun, S.M. Yoon, G.Y. Lee, J.P. Choi, J.S. Lee, Mater. Trans. **55**, 1630 (2014).
[11] C.B. Song, T.R. Cho, Korean J. Mater. Res. **8**, 720 (1998).
[12] S.S. Jung, Y.S. Kang, J.S. Lee, Mater. Sci. Forum **534-536**, 153 (2007).
[13] J.C. Yun, G.Y. Lee, J.S. Lee, Kor. J. Met. Mater. **48**, 995 (2010).
[14] H. Nakamura, S. Sugimoto, T. Tanaka, M. Okada, M. Homma, J. Alloys Compd. **222**, 13 (1995).
[15] A. Verma, R.K. Sidhu, S. Mahajan, O.P. Pandey, J. Mater. Sci. Lett. **15**, 2088 (1996).
[16] H. Fujii, M. Akayama, K. Nakao, K. Tatami, J. Alloys Compd. **219**, 10 (1995).
[17] O. Isnard, S. Miraglia, M. Guillot, D. Fruchart, J. Appl. Phys. **75**, 5988 (1994).
[18] J.E. Shield, D.J. Branagan, C.P. Li, R.W. McCallum, J. Appl. Phys. **83**, 5564 (1998).
[19] B.D. Cullity, C.D. Graham, Introduction to magnetic materials, John Wiley & Sons, New Jersey (2011).
[20] J.G. Lee, S.W. Kang, S.J. Park, Y.W. Oh, C.J. Choi, Kor. J. Met. Mater. **48**, 842 (2010).
[21] T. Saito, H. Arimitsu, K. Nakajima, Y. Iwase, H. Shima, United States Patent, US 5190627 (1993).
[22] T. Konishi, H. Nagai, Y. Nakata, T. Okutani, J. Magn. Magn. Mater. **269**, 48 (2004).
[23] E.S. Yoon, Ph.D. Thesis, Hanyang University (2002).
[24] C.J. Yang, W.Y. Lee, S.D. Choi, Mater. Sci. Eng **181-182A**, 1010 (1994).